Published in PIANC Bulletin, nr 114, Oct 2003, pp 53-63
ISSN 0374-1001

Bowtruster-induced damage

L.A. Schokking Delft University of Technology and Ministry of Public Works, Road and Hydraulic Engineering Division
P.C. Janssen Ministry of Public Works, Road and Hydraulic Engineering Division
H.J. Verhagen Delft University of Technology

Keywords: Bowthruster, stone stability, scour, jet wash, quays
Mot-clefs: Propulseurs d'étrave, stabilité de moellon, épaufrure, lessivage par jet, quai

Introduction

The stability of stones in propeller-induced jet wash is still difficult to predict. Especially the trend of bowthrusters increasing in size and power in sea going ships (especially ferries) over the last years may be a reason for concern when dealing with the protection of slopes and beds.
But also ships used in inland navigation are using bowthrusters more intensively. Because of high costs of crew, many inland navigation ships try to sail with a minimum of crew. In order to allow mooring with a limited number of staff, the manoeuvrability of the ship has to be improved, which is often done by making a bowthruster in the ship. At this moment near mooring dolphins in the navigable rivers of the Netherlands managers are confronted with damage to the slope protection because of heavy use of bowthrusters

In 1997 PIANC has published the "guidelines for the design of armoured slopes under open pile quay walls" (PIANC 1977). In these guidelines a very rough method is described for the determination of the size of rock on slopes under attack by propeller induced currents. Basically the method is as follows:

1. Determine the power and the diameter of the bowthruster of the design ship.
2. Given these values, determine the initial jet velocity flowing out of the bowthruster (u_0).
3. Determine the height of the bowthruster above the bed (z_b).
4. Determine the ratio u_0/u_m from a presented graph
5. When the slope is in a zone $4\ z_b<x < 10\ z_b$ use the found velocity u_m.
6. Read the required stone size from a graph, and increase the value with 50% because you are on a slope.

Application in recent years has shown that this method is not very reliable, and subject to much discussion. Especially because the determination and stability calculation can be done with much more accuracy.

From these the conclusion can be drawn that it is necessary to improve design formulas for the effect of a bowthruster, as also suggested by Römisch and Hering (2002). The second step is then to make a conceptual model of the effect of (propeller-induced) turbulence on the stability of the slope, followed by a systematic set of tests in the lab in order to verify the conceptual model and in order to determine the calibration constants in the conceptual model.

Therefore, Delft University of Technology started a research program to investigate the effects of bowthrusters in particular. As part of this program two different types of investigations have been carried out in cooperation with the Dutch Ministry of Transport, Public Works and Water Management:

- The stability of stones in propeller-induced jet wash on a slope was investigated using an experimental model at Delft University of Technology (DUT).
- The scour effects of bow- and mainthrusters in Dutch inland waterways were investigated in a case study in the Amsterdam-Rijnkanaal, a 70 kilometre long artificial channel leading from Amsterdam to Tiel.

The experimental model

In order to make a physical model of a bowthruster, a decision has to be made on the type of model to be used. Bowthrusters can be modelled in several ways. Basically there are three ways to do this:

1. by using a plain water jet
2. by using a free propeller
3. by using a ducted propeller

Since most bowthrusters are situated in a duct in the bow of the ship it seems obvious to use the third model. However, applying a plain water jet as a model for a propeller in a duct would be a more economic option and therefore it was considered interesting to see whether the results derived from the different types of models differ much concerning stability of stones in the jet wash and velocity field distributions. Should the results appear to be similar, it would be possible to apply a simple, cheap model with a plain water jet.

Van Veldhoven (2002) investigated the difference between the effects of the plain water jet and the ducted propeller jet (model 1 and 3) at DUT. Schokkink (2002) has investigated the free propeller. Van Veldhoven concluded that a free water jet could not be used to physically model a bowthruster since the results concerning the relation of initial velocity and stability of stones on a slope differed largely between the two systems. This paper focuses on the difference between the effects of a ducted propeller and a free propeller of which the results are treated in this paper. The model used was the same as used by Van Veldhoven (2002).

After a short discussion on the set-up of the model and the flow differences in ajet from a free and from a ducted propeller, this paper will focus especially on the stability of stones under influence of such a jet.

Free propeller jet

The tests were conducted at the laboratory of fluid mechanics as DUT. The dimensions of the model are shown in table 1. Since the model was only meant to derive insight in different types of modelling, the hull of the 'ship' was modelled by merely a wooden board from bottom to surface. Figure 7 shows a picture of the model.

Variable	Symbol	Value
Water depth	h_w [m]	0.48
Slope ratio	m [-]	1:3
Maximum beam of vessel	W [m]	1.28
Draught of vessel	h_d [m]	0.44
Keel clearance	h_k [m]	0.04
Height of propeller axis above bottom	z [m]	0.19
Length of duct (ducted propeller only)	L_d [m]	0.30
Distance from duct exit to slope	L [m]	1.16
Diameter of propeller (bow)	D [m]	0.10
Diameter of hole in board (free propeller only)	Db [m]	0.20
Power of bowthruster	P [kW]	30.7
Number of blades on propeller	n_b [-]	4
Rotation rate	n [rpm]	1342
Initial velocity	U_0 [m/s]	1.36
Minimum median stone diameter	d_{50} [m]	0.009

table 1, dimensions of the model

To prevent circulation as much as possible, the water could flow away freely over both sidewalls, which was compensated by an inlet at the backside of the propeller.

Figure 1 shows the geometry of the model.

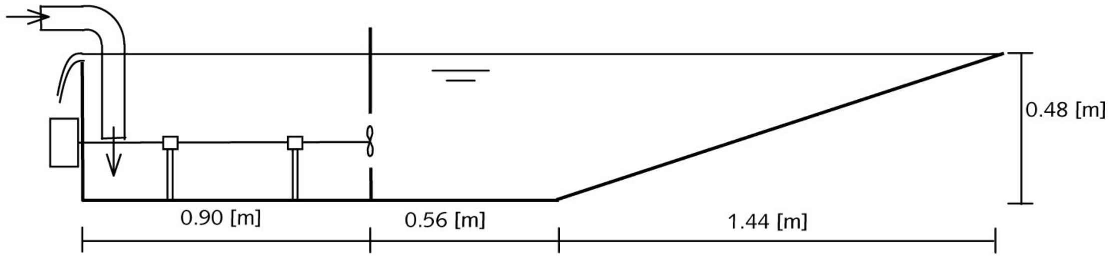

figure 1, side view and dimensions of the free-propeller model.

Measurements

To compare the velocity fields induced by the ducted and free propeller, velocity measurements were performed using an EMS (Electro Magnetic velocity Sensor) with a size of approx. 3 cm. These measurements were taken between 0.5 D $< x <$ 7 D at $y = 0$ and varying the height between –0.2 [m] $< z <$ 0.20 [m].

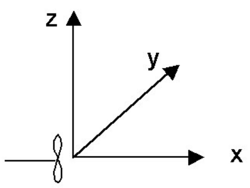

figure 2, definition of the axis

For x = D, 3D and 7D the results are shown in figure 3 in combination with the results of the ducted propeller jet derived by Van Veldhoven (2001). Ux denotes the velocity in x-direction, U0 denotes the initial velocity at the propeller.

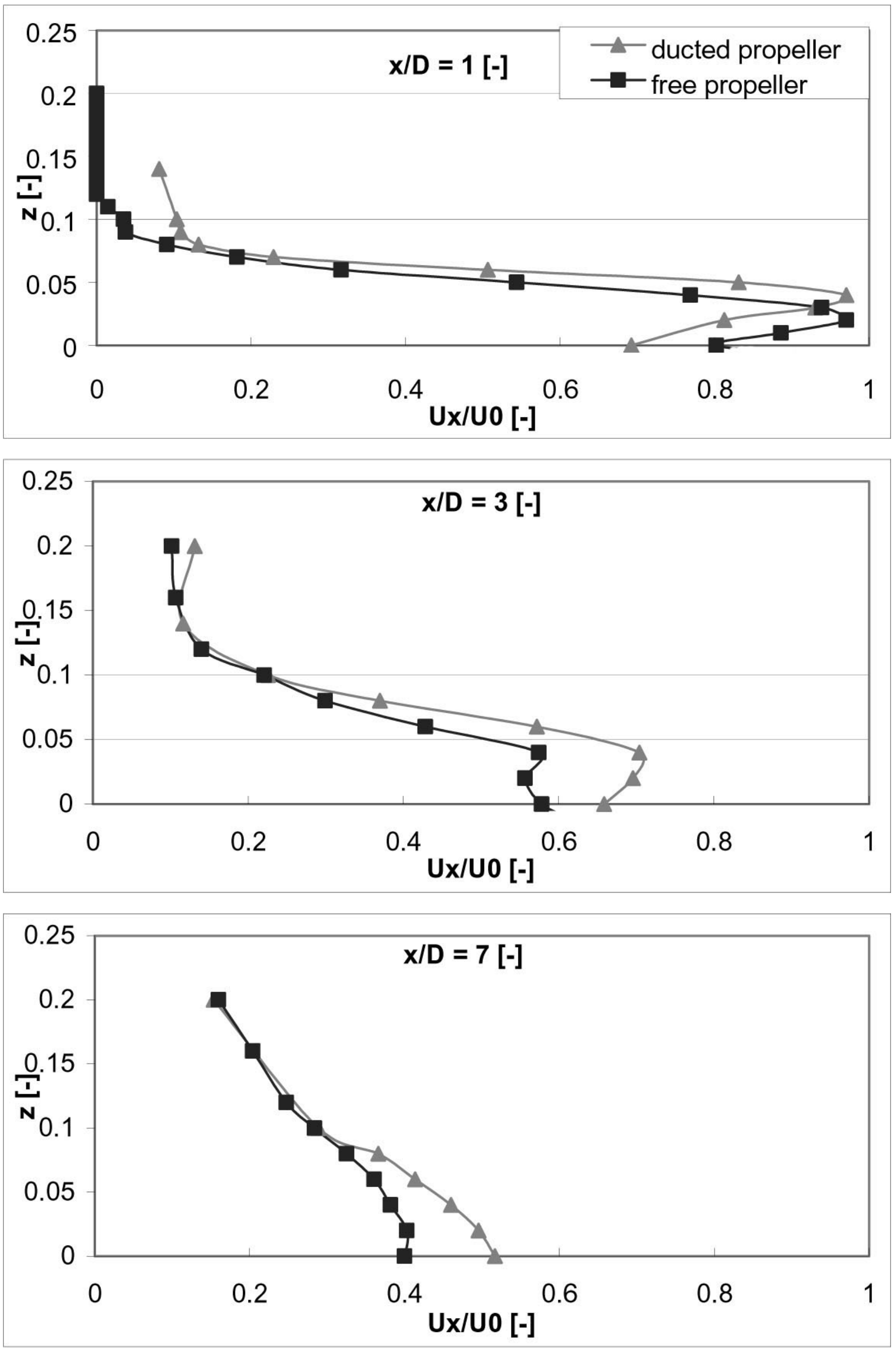

figure 3, velocity profile of the free and ducted propeller jet.

Figure 3 shows that the initial velocity profiles are quite similar. Figure 3 also shows that the velocities in the free propeller jet die down faster in x-direction than the velocities in the ducted propeller jet do.

The explanation for this different behaviour in velocity reduction can be found in the development of the axial relative turbulence development along the x-axis in x-drection, defined as r_x.

$$r_x = \frac{\sqrt{\overline{U_x'^2}}}{\overline{U}_{x,z=0}} \quad [-] \tag{1}$$

where

U_x': fluctuation of the velocity in x-direction [m/s]

$\overline{U}_{x,z=0}$: the mean velocity on the x-axis [m/s]

The relative axial turbulences for the ducted propeller jet and the free propeller jet are shown in figure 4.

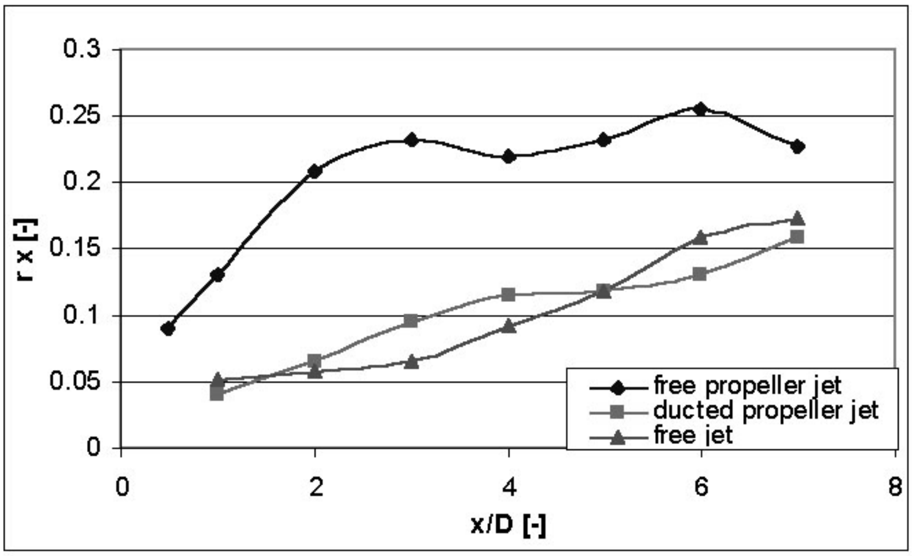

figure 4, axial relative turbulence of free and ducted propeller, and of the plain water jet.

Both the velocity distribution and the relative turbulence for a free propeller jet differ from those for a ducted propeller jet, which is expected to be the most accurate model of a bowthruster. This indicates that probably a bowthruster is not very well modelled by a free propeller.

However, since we are not specifically interested in the flow pattern itself, but mainly in its effects on stone stability, tests were performed to investigate damage due to both propeller jets.

Stones with a diameter of 0.9 [cm] were applied to a slope with a ratio of 1:3 [-] in squares of 5 [cm] by 5 [cm] in 9 different colours, see also figure 7. In that way, movement of a stone and also its origin could be determined leading to the relations between damage (i.e. number of stones moved) and rotation rate, see figure 5.

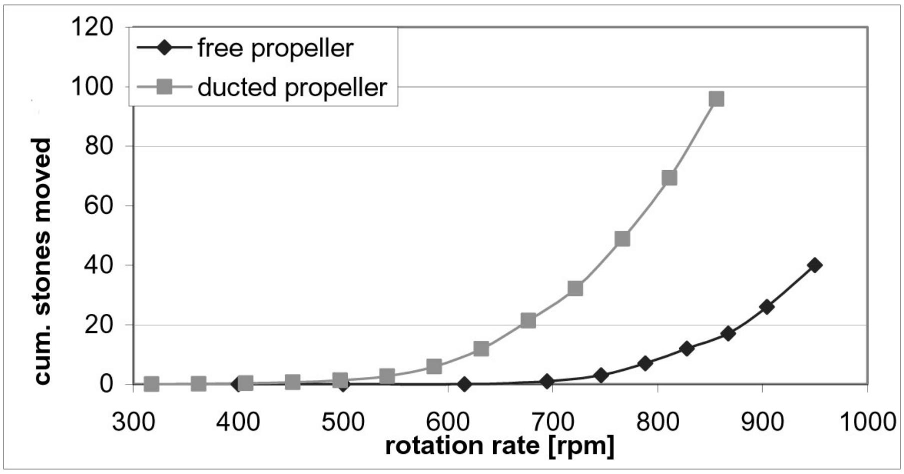

figure 5, damage on the slope related to the rotation rate of the free and ducted propeller jet.

It is noted, however, that the relation between damage and mean velocity in directly in front of the slope is almost the same for both models (free and ducted propeller), see figure 6.

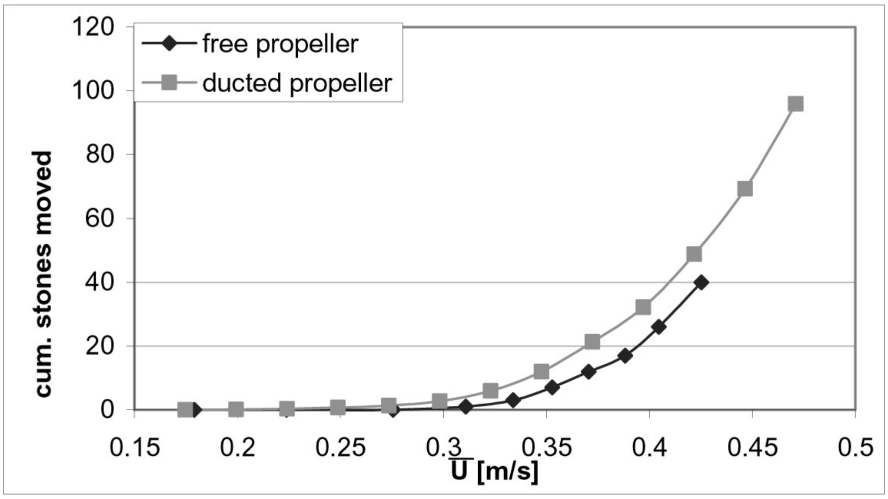

figure 6, damage on the slope, related to the velocity of the free and ducted propeller jet in front of the slope.

The results described above can be explained by the difference in turbulence between the two systems:

Due to higher turbulence in the free propeller jet the velocity decreases faster in space leading to less damage on the slope than in case of the ducted propeller jet. The fact that in this case the turbulence in the free propeller jet is higher just in front of the slope than it is in the ducted propeller jet does not seem to make a difference concerning the stability of stones on the slope.

Damage location

The area of the damage is a point of interest, since slopes are usually protected using (expensive) stones, which one only wants to apply where necessary. In both tests (the ducted and the free propeller jet) the damage appeared to occur at the lowest part of the slope, i.e. the toe of the slope. The jet axis however, where the highest velocities are expected, intersects with the slope a lot higher, see figure 7.

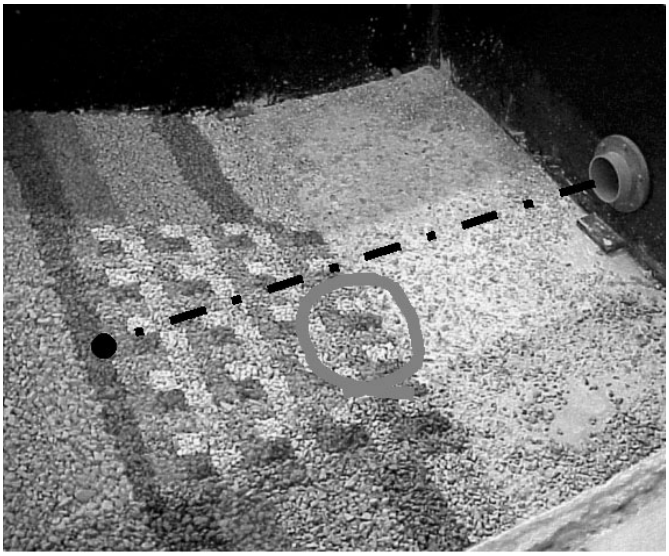

figure 7, damage location on the slope (circle) in the ducted propeller model and the intersection of the jet-axis with the slope (black dot).

A second series of tests was conducted to determine the cause of this phenomenon. Velocity measurements in all three directions were carried out in the area above the slope (using an EMS again).

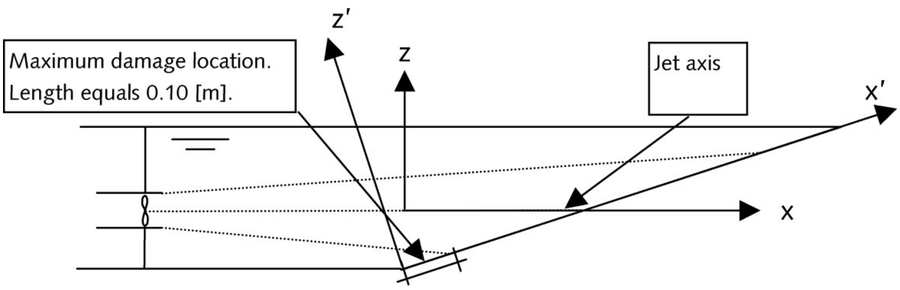

figure 8, definition of axis and location of damage.

Measurements show that the velocities in x-direction are largest everywhere in the axis of the jet, i.e. at z = 0. Figure 9 shows the average velocity parallel to the slope, i.e. in x'-direction, 0.025 [m] above the slope. Along the slope the velocities are largest at x' = 0.6 [m], i.e. where the jet axis intersects with the slope. Since the damage occurs lower on the slope, this means that the average velocity cannot directly be related to the occurring damage.

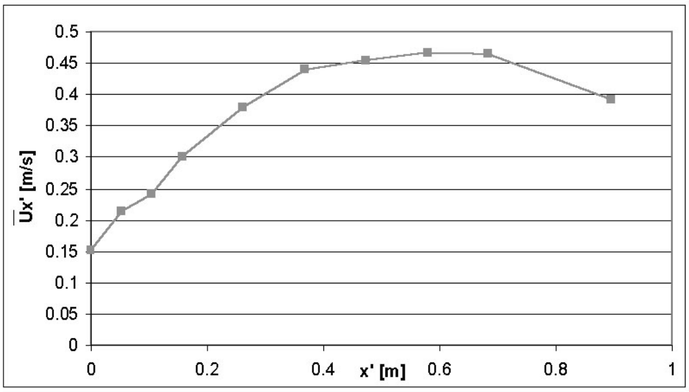

figure 9, average velocities parallel to the slope.

The calculated peak velocities (Schiereck 2001) along the slope are shown in figure 10.

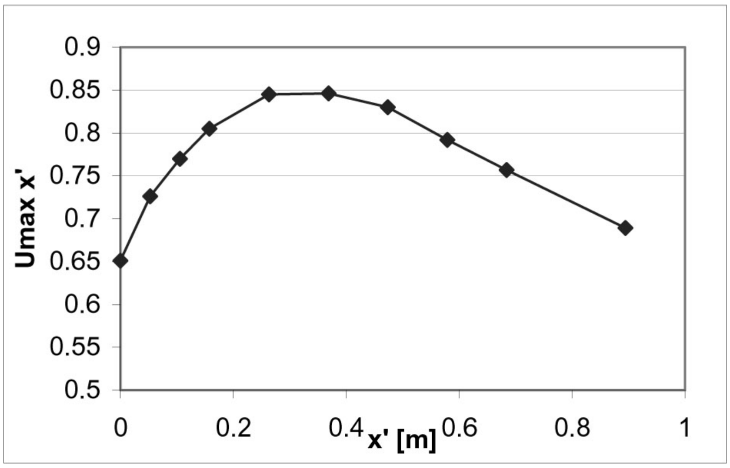

figure 10, peak velocities parallel to the slope.

Clearly, the peak velocities cannot directly be related to occurring damage either.

A stone is moved by a combination of acting forces. In this case two forces can be distinguished, a shear force and a pressure force. The shear force is related to the peak velocities acting on the stone, the pressure force is induced by accelerating or decelerating water.

Figure 10 also shows that in this case there is a considerable convective acceleration (i.e. an acceleration in space) along the lower part of the slope. This means that for an individual stone, the velocity in front of the stone (left side in this case) is higher than on the backside of the stone, which is shown in figure 11.

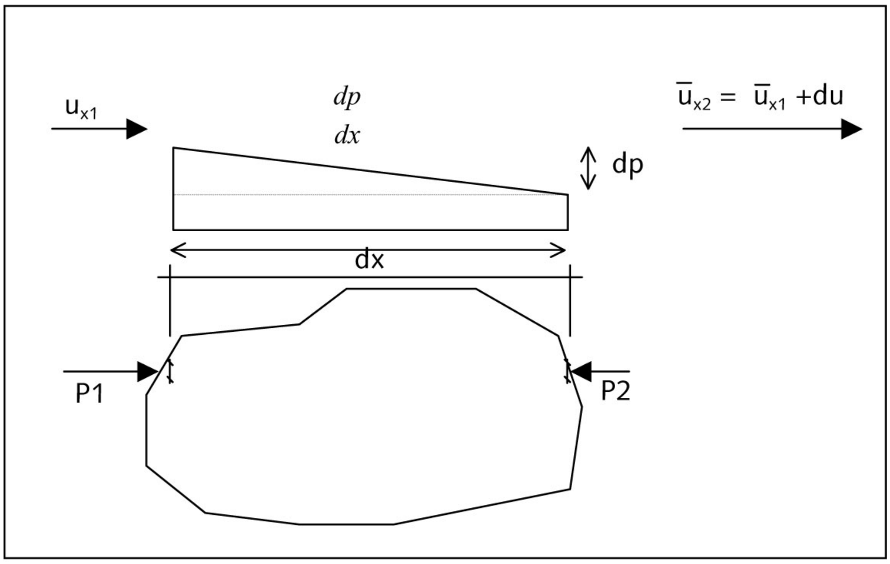

figure 11, velocity difference over a stone.

Applying Bernoulli's theorem, the pressure force that acts on each stone on the lower part of the slope is equal to

$$F_p = V \cdot \frac{dp}{dx} \quad [N] \qquad (2)$$

where:

F_P:	Pressure force [N]
V :	Volume of the particle [m^3]
$\frac{dp}{dx}$:	Pressure difference over a stone per unit length, constant [$N/m^2/m$]

It is noted that equation 2 is valid under the assumption that du/dx = constant over the length of a stone, which is correct here since the dimensions of the stone are relatively small.

For the shear stress the following equation is commonly used:

$$\tau = \rho_w \cdot u^{*2} \quad [N/m^2] \qquad (3)$$

where:

τ:	shear stress [N/m^2]
u^*	shear velocity [m/s] ($= u \cdot \frac{\sqrt{g}}{C}$)
C:	Chézy constant [$m^{1/2}/s$] (= 18 log (12·h/k))
h :	water depth [m]
k :	roughness of the bed, equals 2 to 3 times the d_{50} [m]

Figure 12 shows the shear force and pressure force acting on a stone with a diameter of 0.9 [cm].

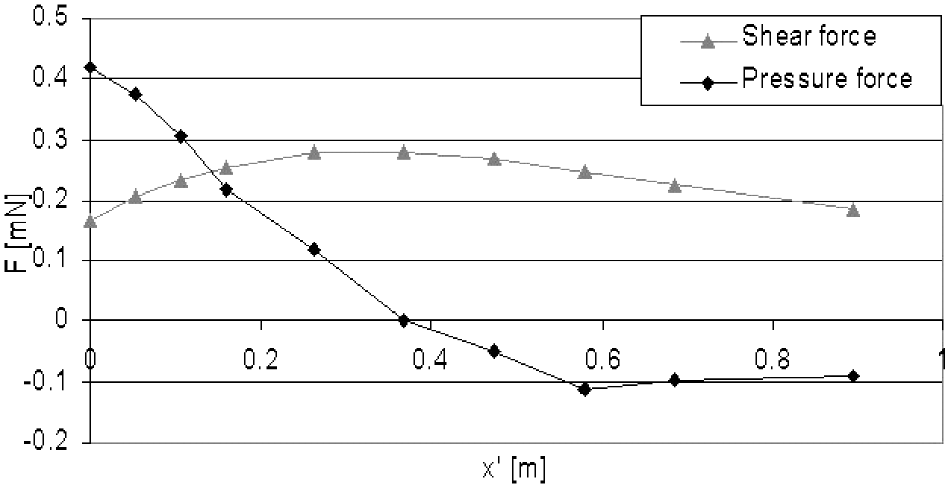

figure 12, shear force and pressure force acting on a stone.

At the lower part of the slope the combined forces are largest, explaining the location of the maximum damage, at the toe of the slope.80

Conclusions from the tests for design applications

As stated before, the maximum damage is not at the point of the maximum velocity, but at a much lower location. This seems to be caused by the gradients in the pressure force. For practical design it means that in design formula for the stability of stones on a slope under influence of a jet, one cannot neglect this effect.
Because the tests were on small scale only, upgrading the results to prototype scale in a quantitative way is rather difficult. It is unclear if the model propeller produces the turbulence in the jet “on scale” related to a prototype propeller. However, it is obvious that in a design formula the acceleration effect as well as the propeller turbulence have to be included. It seems not to be appropriate to apply a shields-type of formula using the average flow velocity from a free jet plus one single bulk correction factor.

Case study Amsterdam-Rijnkanaal

To derive insight in the present bowthruster related scour problems a field study was conducted in the Amsterdam-Rijnkanaal. Since bowthrusters are mainly used during berthing and unberthing, only the scour patterns along quay walls at berthing facilities were investigated.
Different scour patterns were found, depending on the geometry of the quays. It appeared that two different kinds of quays could be distinguished (in the Amsterdam-Rijnkanaal), based on their geometrical differences, viz.:

1. Long quays (L > 300 [m]) with no distinct geometrical anomalies, and
2. short quays (L < 300 [m]) or quays with distinct geometrical anomalies.

In this paper, the first type is referred to as a uniform quay, the second type is referred to as a non-uniform quay. As mentioned, the scouring pattern is found to be different at these quays.
The reason is found to be the following phenomenon: at uniform quays ships berth randomly, both location wise and direction wise. This means that the hydraulic load from the bow- and mainthruster is on a different location each time a ship berths. Since scour is a time dependent phenomenon, it has no time to fully develop at uniform quays, leading to relatively shallow and widespread scour. At non-uniform quays the ships tend to berth more consistently, leading

to a hydraulic load from bow- and mainthruster at approximately the same spot each time a ship berths. Consequently, it is expected that at non uniform quays the scour has time to fully develop, leading to larger and more concentrated scour holes than at uniform quays.

In the following paragraph an example of both a uniform and a non-uniform quay is treated. The findings on scourdepths will be substantiated by a theoretical analysis based on Römisch (1977), adapted by Dücker and Miller (1996).

Examples

Figure 13 shows the bathymetry along a uniform quay, at the village of Maarssen. The scour is widespread and shallow (h < 1 [m]). Only at a few points scour occurs immediately in front of the sheetpile construction, so there is no reason for concern for the stability of the sheetpiles. Because of the irregularity in berthing it is not possible to make a distinction between bowthruster-induced scour and mainthruster-induced scour at such a uniform quay.

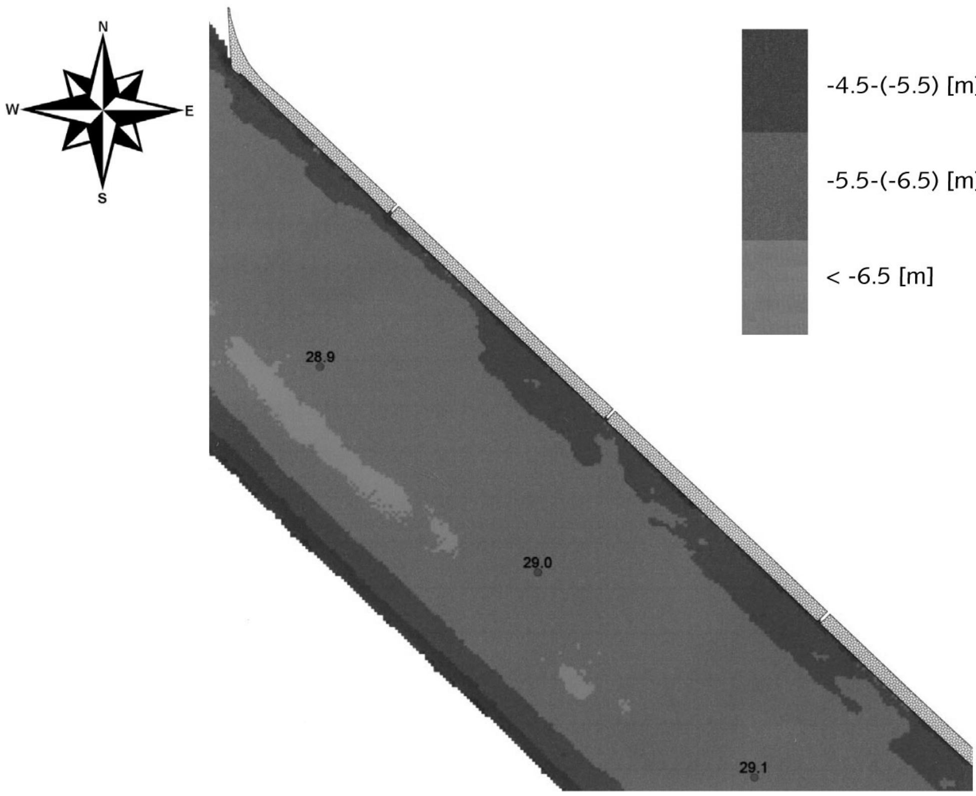

figure 13, bathymetry at Maarssen.

Figure 14 shows the bathymetry at a non-uniform quay, at the so-called 'Plofsluis' near the town of Nieuwegein in this case.

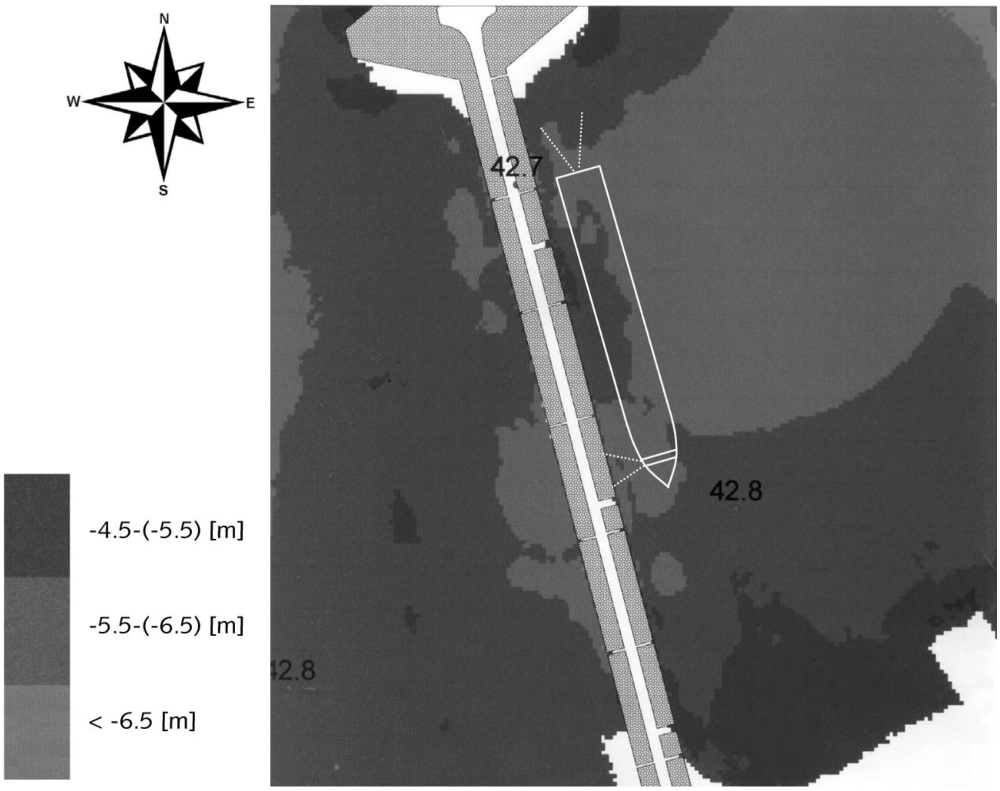

figure 14, bathymetry at the Plofsluis.

The focus will be on the east side of the quays. Clearly two scour holes can be distinguished.

The following hypothesis on the way that ships berth may explain the location and development of these holes:
When ships approach from the south, the easiest berthing is at the south side of the Plofsluis or a little further to the north at Houten at the east side of the canal. When coming from the north it is easiest to berth at the north side of the Plofsluis, as far to the north as possible, for easy unberthing. This would lead to a frequently occurring position of ships as shown in figure 14, which explains the development of the two scour holes, one due to mainthruster use, one due to bowthruster use.

The maximum scour depths related to bowthruster and to the mainthruster are approximately 1.3 [m] and 1.7 [m] respectively. This indicates that bowthrusters are capable of inducing scour in the same order of magnitude as mainthrusters do.

Apart from these quays, several others have also been investigated and similar conclusions could be drawn.

Comparison with theory

Measured scour depths have been compared to theoretical values, based on the theory of Römisch (1977), adapted by Dücker and Miller (1996):

$$\frac{h_{hole}}{d} = C_m \cdot 0.1 \cdot \left(\frac{B}{B_{crit}} \right)^{13} \quad for\ 1.0 < \left(\frac{B}{B_{crit}} \right) < 1.4\ [-] \tag{4}$$

$$\frac{h_{hole}}{d} = C_m \cdot 4.6 \cdot \left(\frac{B}{B_{crit}} \right)^{2.25} \quad for\ \left(\frac{B}{B_{crit}} \right) > 1.4\ [-] \tag{5}$$

where

h_{hole}:	depth of the hole [m]
B:	Parameter of Römisch [-] (1977) $\left(= \frac{U_{\max,bot}}{\sqrt{\frac{\rho_s - \rho_w}{\rho_w} \cdot g \cdot d}} \right)$
B_{crit}:	constant [-] (1.25)
C_m :	constant [-] (0.3 for manoeuvring ships, 1.0 for ships at rest)
d:	diameter of the grain [m]

For the coefficient C the value of 0.3 [-] is taken, which should be used for manoeuvring ships. This leads to the following measured and calculated scour hole depths for the quays near Maarssen and near the Plofsluis.

Maarssen	Dücker and Miller C = 0.3 [-]	Measured (in front of quay)
Bowthruster	2.3 [m]	0.9 [m]
Mainthruster	3.4 [m]	

table 2

Plofsluis	Dücker and Miller C = 0.3 [-]	Measured (in front of quay)
Bowthruster	1.4 [m]	1.3 [m]
Mainthruster	2.2 [m]	1.7 [m]

table 3

The values presented in table 2 show that at Maarssen the calculated values are too high. This is logical, since the scour has no time to develop at uniform quays, as mentioned before. At the Plofsluis (table 3) measured and calculated values for both mainthruster and bowthruster-induced scour differ only slightly. This leads to believe that at these locations the scour is practically fully developed, complying with the expectation of non-uniform quays.

Conclusions

This research was conducted to 1) derive insight in the correct method of modelling a bowthruster, 2) to explain the way in which damage on a slope occurs and 3) to get an idea of practical problems in inland waterways concerning bowthruster-induced scour.

Firstly, it is concluded that a bowthruster should be modelled using a propeller in a duct. Without the duct, or when using a plain water jet, the results concerning stability of stones in the jet differ largely from results derived with a propeller in a duct.

Secondly, the initiation of movement was found to be caused by a combination of shear force and pressure force along the slope. The shear force is related to the peak velocities, the pressure force to the convective acceleration induced by the peak velocities. The pressure force proved to be quite dominant on the lower part of the slope.

Finally, In the Amsterdam-Rijnkanaal some berthing places were found that showed a difference between bowthruster-induced scour and mainthruster-induced scour, which can be distinguished tanks to the regularity in berthing at these locations, the non-uniform quays. Bowthruster-induced scour proved to be of the same order of magnitude as mainthruster-induced scour at the locations investigated. However, no locations were found in the Amsterdam-Rijnkanaal where the bowthruster-induced scour should be considered governing.

Acknowledgements

This study has been done in the framework of general research programme of the department of Hydraulic Engineering of Delft University of Technology. The test were executed in the Laboratory of Fluid Mechanics of the Delft University. Supplementary funding was provided by the Ministry of Public Works, Road and Hydraulic Engineering Division in Delft.

References

Schiereck, G.J.(2001) *Introduction to bed, bank and shore protection*, Delft University Press, The Netherlands, ISBN 90.407.1683.8

Veldhoven, V., van, (2002)*Vooronderzoek schroefstraal op een talud met breuksteen*, M.Sc-thesis, Delft University of Technology

Fuehrer, M; Romisch, K., *Effects of modern ship traffic on inland- and ocean waterways and their structures,* 24th International Navigation Congress, Leningrad, S.I-3, p. 79-94, 1977

PIANC (1997) Guidelines for the design of armoured slopes under open piled quay walls, *report of working group 22, supplement to Bulletin 96, 38 pp*

K. Römisch and W. Hering (2002) Input data of propeller induced velocities for dimensioning of bed protection near quay walls - a comment on existing recommendations*, PIANC Bulletin 109, January 2002*

Schokking, L. (2002) *Bowthruster induced Damage*, M.Sc.-thesis, Delft University of Technology

Abstract

The influence of bowthrusters was investigated in two ways in this paper:
Firstly, an experimental model was used to show that a bowthruster should be modelled by a propeller in a duct, and a simplification of the prototype by a free jet or by a non-ducted propeller is not possible. It was also shown, that the damage on a slope occurs at the lowest

part of this slope, even though the jet-axis, carrying the largest velocities, intersects with the slope a lot higher. The reason for it is found to be the fact that a convective acceleration exists on the lowest part of the slope, leading to a dominant pressure gradient at that location.
Secondly, (apart from the experimental investigation), a field study was performed in the Amsterdam-Rijnkanaal to see what the effects of bowthrusters are in inland waterways. It appears that at long, straight quays the scour tends to be shallow and widespread. This is explained by the combination of the fact that ships berth randomly at these quays, location and direction wise, and the fact that scour is a time dependent phenomenon. It was also found, consequently, that quays that are either short, or quays with geometrical anomalies lead to consistent berthing of vessels, which leads to the development of deeper, concentrated scour holes.

Résumé
L'effet des propulseurs d'étrave a été étudié de deux manières dans ce rapport. Premièrement, un modèle physique a montré qu'un propulseur devait être modélisé par une hélice dans un tube et que la représentation par un jet libre ou par une hélice sans tube ne convenait pas. Il est apparu que le dommage sur un perré se produit en pied de talus même si l'axe du jet, lieu des vitesses les plus fortes, touche le perré bien au dessus. La raison tient a l'existence d 'une accélération convective en pied de talus conduisant a un gradient de pression maximum en ce point.
Deuxièmement (outre la recherche sur modèle) une étude a été menée dans le canal du Rhin à Amsterdam pour voir les effets des propulseurs en navigation fluviale. Il apparaît sur des quais en alignement et de grande longueur, que l'épaufrure tend à remonter prés de la surface et a s'allonger. Cela s'explique par la combinaison de deux facteurs, le fait que les bateaux accostent de manière aléatoire le long de tels quais en position comme en orientation et le fait que l' épaufrure est fonction de la durée d'attaque. Ainsi a t on pu observer que les quais courts ou présentant des particularités de tracé font l'objet d'accostages beaucoup plus identiques, ce qui conduit à des dégradations plus profondes et plus localisées.

Zusammenfassung
Der Einfluss von Bugstrahlrudern wurde auf zweierlei Weise untersucht. Zum einen konnte mit Hilfe eines experimentellen Modells gezeigt werden, dass ein Bugstrahlruder mittels eines Propellers in einer Rohre modelliert werden sollte und dass eine Vereinfachung des Prototyps durch einen freien Strahl oder einen Propeller ohne Röhre nicht möglich ist. Es konnte zudem gezeigt werden, dass der Schaden an einer Böschung am untersten Böschungsteil auftritt, selbst wenn die Strahlachse, die die höchsten Strahlgeschwindigkeiten aufweist, an einem höheren Punkt der Böschung auftrifft. Der Grund dafür liegt in der Tatsache, dass am untersten Böschungsteil eine konvektive Beschleunigung auftritt, verbunden mit einem dominanten Druckgradienten an dieser Stelle.

Zum anderen wurde ein Feldversuch im Amsterdam-Rijnkanaal durchgeführt, um die Auswirkungen von Bugstrahlrudern in Binnenwasserstraßen zu untersuchen. Es zeigte sich, dass an langen, geraden Kais eine Tendenz zur Ausbildung von flachen, ausgedehnten Kolken besteht. Dies hat seine Ursache darin, dass die Schiffe an diesen Kais in Bezug auf Ort und Richtung zufällig verteilt festmachen und dass Kolkbildung ein zeitabhängiges Phänomen ist.
Es zeigte sich daher auch, dass eher kürzere Kais oder Kais mit geometrischen Anomalien zu einem einheitlichen Ankern der Schiffe führen, verbunden mit der Ausbildung tieferer und lokal konzentrierter Kolke.